This is the post-print version of an article finally published as:
Díaz-López T, Lages-Gonzalo M, Serrano-López AM, Alfonso C, Rivas G, Díaz-Orejas R, Giraldo R (2003) Structural changes in RepA, a plasmid replication initiator, upon binding to origin DNA. *J. Biol. Che*m. **278**: 18606-18616. Doi:10.1074/jbc.M212024200

# Structural Changes in RepA, a Plasmid Replication Initiator, upon Binding to Origin DNA

**Teresa Díaz-López[†], Marta Lages-Gonzalo[†§], Ana Serrano-López[†], Carlos Alfonso[#], Germán Rivas[§,#], Ramón Díaz-Orejas[†], and Rafael Giraldo[†*]**

Departments of Molecular Microbiology† and Protein Structure and Function§, and Analytical Ultracentrifugation Facility#.
Centro de Investigaciones Biológicas, Consejo Superior de Investigaciones Científicas (CSIC).
C/ Velázquez, 144. 28006 Madrid. SPAIN

*To whom correspondence should be addressed. Tel: 34-91-5611800; Fax: 34-91-5627518; E-mail: rgiraldo@cib.csic.es

**RUNNING TITLE:** Binding to iteron DNA changes RepA structure

## SUMMARY

RepA protein is the DNA replication initiator of the *Pseudomonas* plasmid pPS10. RepA dimers bind to an inversely-repeated operator sequence in *repA* promoter, thus repressing its own synthesis, whereas monomers bind to four directly-repeated sequences (iterons) to initiate DNA replication. We had previously proposed that RepA is composed of two Winged-Helix (WH) domains, a structural unit also present in eukaryotic and archaeal initiators. In order to bind to the whole iteron sequence through both domains, RepA should couple monomerization to a conformational change in the N-terminal WH, which includes a Leucine-Zipper (LZ)-like sequence motif. We show for the first time that, by itself, binding to iteron DNA *in vitro*: i) dissociates RepA dimers into monomers and ii) alters RepA conformation, suggesting an allosteric effect. Furthermore, we also show that similar changes in RepA are promoted by mutations that substitute two Leu residues of the putative LZ by Ala, destabilizing the hydrophobic core of the first WH. We propose that this mutant (RepA-2L2A) resembles a transient folding intermediate in the pathway leading to active monomers. These findings, together with the known activation of other Rep-type proteins by chaperones, are relevant to understand the molecular basis of plasmid DNA replication initiation.

**ABBREVIATIONS**

*bis-ANS*, 4,4'-dianilino-1,1'-binapthyl-5,5'-disulfonic acid;

*CD*, Circular Dichroism;

*EMSA*, Electrophoretic Mobility Shift Assay;

*EtBr*, Ethidium Bromide;

*His6*, Hexahistidine tag;

*HTH*, Helix-Turn-Helix;

*Kn*, Kanamycin;

*LZ*, Leucine Zipper;

*MBP*, Maltose Binding Protein;

*OD*, Optical Density;

*ORC*, Origin Recognition Complex;

*WH*, Winged Helix;

## INTRODUCTION

DNA replication is a tightly regulated process in order to guarantee that genetic information is precisely copied once, and only once, each cell cycle (1). This is achieved by means of complex circuits that are distinct in prokaryotes and eukaryotes, although recently some similarities have become evident (2-4). Common essential elements are a *cis*-acting DNA sequence (the origin of replication) and a *trans*-acting factor (the initiator). DNA replication initiators are single proteins, or multisubunit complexes, that bind specifically to the origin of replication, where they usually assemble into oligomers. Initiators play two roles: i) to melt the strands of DNA and ii) bring to the so-created replication bubble a number of other protein factors. These are required for further extension of the replication fork (helicases), synthesis of an RNA primer (primases) and copying the template (DNA polymerases) (reviewed in 1,2). Any initiator, to be enabled to bind and melt origin DNA, requires an activation step whose molecular basis is a central subject in research on both DNA replication and the cell cycle.

A trait common to initiators is that their function is controlled by ATP binding and hydrolysis (3,5,6) defining active or silent conformational states. In the bacterial chromosomal initiator, DnaA (reviewed in 7), ATP is not strictly required for specific binding to double-stranded origin DNA (*oriC*). However, it is essential for melting *oriC* AT-rich repeats, binding to the resulting single-stranded sequences (6) and then for loading DnaB helicase. Subsequent ATP hydrolysis, stimulated by the processivity factor of DNApol III (β-clamp) and other cellular factors, renders DnaA unable to initiate further replication rounds. DnaA can then be re-activated either by acidic phospholipids or DnaK chaperone, that exchange ADP by ATP (7). On their side, Orc1 and Orc5 subunits of the eukaryotic initiator ORC also bind ATP which is required for specific recognition of origin sequences (8). Single-stranded

DNA, generated after origin melting, stimulates ATP hydrolysis and exerts a change in the overall shape of ORC (5).

Plasmids are extrachromosomal DNA molecules that borrow from their hosts most of the factors required for replication. However, they often encode their own initiator, termed Rep (reviewed in 9,10). In Gram-negative bacteria, Rep proteins usually bind to directly-repeated sequences (iterons) to establish the initiation complex. In addition, some Rep proteins also bind to an inversely-repeated sequence (operator) that overlaps with the promoter of the *rep* genes, thus acting as self-repressors. Dimers of Rep bind to the operator, whereas monomers bind to the iterons (11-17).

RepA is the initiator protein of pPS10, a plasmid isolated from *Pseudomonas* (18). Mutations in a LZ-like sequence motif, found at the N-terminus of RepA (19), enhance dimer dissociation (14). However, a proof for a direct role of LZ in RepA dimerization is still lacking. An HTH motif at the protein C-terminus is the main determinant of RepA binding to both operator and iteron DNA sequences (20). We have recently proposed (21) that RepA consists of two WH domains (reviewed in 22). Furthermore, a similar WH fold is found at the C-terminus of the eukaryotic/archaeal initiators Orc4/Cdc6 (4,23), underlining the relevance of studying the molecular mechanism of RepA activation. We had proposed that dissociation of RepA dimers into monomers would result in a structural change altering the relative arrangement and compaction of its two WH domains (21). In the dimers, the C-terminal domain (WH2) binds to the operator through the major groove, whereas the N-terminal domain (WH1) acts as dimerization interface. In the monomers, WH2 binds to iteron DNA as does to the operator, while the remodelled WH1 binds to the 5´ end of iteron through both the phosphodiester backbone and the minor groove (21). This model has been then confirmed by the crystal structure of the monomer of a related initiator, RepE54, bound to iteron DNA (24). It shows that the α-helix that might resemble a LZ in the dimers is found in the monomers

split into two helical portions, packed together and buried in the hydrophobic core of WH1 (24).

A feature of Rep-type initiators is that, opposite to DnaA and ORC, they do not bind ATP. Thus, although Rep proteins can promote some structural transitions in DNA, most plasmids require DnaA to aid in origin melting (17,25-30) and helicase loading (28,29). However, they still experience conformational activation (reviewed in 30). Molecular chaperones, either the triad DnaK-DnaJ-GrpE or ClpA, have been implicated in the activation of the Rep-type initiator proteins of plasmids P1 (11,31-34) and F (35). ClpX chaperone has a role in the activation of the initiator of RK2 plasmid (36). In addition, ClpA unfolds P1 Rep to be proteolyzed by ClpP (37-38). We have recently proposed that Hsp70 chaperones, the eukaryotic homologues of DnaK, are implicated in the assembly of ORC (4). Two alternative functions have been proposed for chaperones in P1 replication: either Rep dimers would be so stable that chaperones are required to dissociate them (31,32), or they would modify Rep conformation (39). Thus, some monomeric mutants still require the action of chaperones *in vivo* (33,34), although they have higher association rates to iterons *in vitro* and increased initiation frequency (40). In addition, dimers of a few Rep-type proteins dissociate spontaneously by dilution (34,41,42). The current view is that chaperones would induce in Rep both monomerization and a conformational change, whose exact nature remains to be determined (30,39,43).

We have searched for determinants of the activation of pPS10 RepA. We show in this paper that micromolar amounts of a single iteron DNA sequence actively induce *in vitro* both the dissociation of RepA dimers into monomers and a conformational change. On the contrary, binding of RepA dimers to the operator sequence neither dissociates them, nor changes their conformation. The ligand-induced monomerization of RepA dimers with a coupled conformational change, reported in this paper, would thus be a case for the allosteric

effect of DNA substrates in the structure of their binding domains (44,45), and a novel player in the activation of plasmid DNA replication initiators. Furthermore, we also present a detailed biophysical characterization of RepA-2L2A, a mostly monomeric species of RepA obtained by site-directed mutagenesis of two Leu residues in the LZ-like motif. Our data suggest that it resembles a transient folding intermediate in the way from dimers to active monomers. In RepA-2L2A, the mutations disable the first of the two α-helical portions of the putative LZ to fold back into the second one, thus disrupting hydrophobic interactions at the core of monomeric WH1.

## EXPERIMENTAL PROCEDURES

*Cloning, Expression and Purification of RepA-2L2A*. His6-RepA-WT was expressed, purified and, when required, its tag removed as previously described (21). Mutant *repA*-2L2A gene was obtained by PCR, using as template the expression vector pRG-*recA*-NHis-*repA*-WT (23) and primers including: i) A *Sac*II site plus sequences coding for the 5´ end of *repA*, but with mutated codons (GCC for Ala12 and GCG for Ala19) replacing those for leucines in the putative LZ. ii) A *Hin*dIII site, plus a TGA stop codon and sequences complementary to the 3´ end of *repA*. Mutations were verified by automated DNA sequencing. Expression of His6-RepA-2L2A was carried out at 30 ºC in *E. coli* SG22097 (*clpXP*), as performed for RepA-WT (21). His6-RepA-2L2A was purified to homogeneity from inclusion bodies using the same procedure developed for deletion mutants in RepA (21). Protein stocks were kept in 0.5 M $(NH_4)_2SO_4$, 50 mM $NH_4$-acetate pH= 6.0, 10 mM β-MeEtOH, 0.1 mM EDTA, 10% glycerol. RepAs concentrations were calculated based on their absorption at 280 nm in 5.6 M GuHCl, considering a molar extinction coefficient of 17210 $M^{-1}cm^{-1}$ (http://www.expasy.ch/tools/protparam.html).

*Testing in P. aeruginosa the Effect of the His6-tag and the 2L2A Mutation in RepA.* pPSEC, a new series of shuttle vectors including the pPS10 and ColE1 replicons, was constructed as follows. pRG9B (46) was digested with *Bam*HI to give a 4 Kbp fragment including the pPS10 replicon (18) and the Kn resistance determinant. This fragment was then filled-in with Klenow and ligated to a 759 bp *Dra*I-*Afl*III (*ori*) fragment from pUC18, in which the later site had also been made blunt-ended. The resulting plasmid (pPSEC1) was then modified to substitute the 5´ half of the *repA*-WT gene (a 317 bp *Eco*RI-*Sph*I fragment) by versions encoding a His6 tag (pPSEC2) and the 2L2A mutations (pPSEC3). This was carried out by PCR on the corresponding pRG-*recA*-NHis-*repA*-WT / 2L2A templates (see above), using as primers: i) A 41 bp tail with the sequence between the *Eco*RI site and the ATG initiation codon in *repA* (18), plus the encoded His6 tag. ii) Sequences from the complementary non-coding strand comprising the *Sph*I site in *repA*. The three pPSEC constructs were rescued in *E. coli* JM109, checked by DNA sequencing and then transformed into *P. aeruginosa* PAO1024 (18). *Relative plasmid copy numbers* were determined from cultures of PAO1024 / pPSECs in LB medium, supplemented with Kn to 50 $\mu$g/ml, at 30 ºC. 1.5 ml aliquots were harvested at $OD_{600}$= 0.5 and total lysates were obtained as described (18). 60 $\mu$l (1/10) of the lysates were then loaded into 0.8% agarose-TAE gels, run at 30 V for 12.5 h and stained with EtBr. Southern blotting was carried out by transferring the gels to nylon membranes (18), then hybridized with a 954 bp *Eco*RI *repA* fragment from pRG9B, radiolabelled by random priming with Klenow and 40 $\mu$Ci of [$\alpha$-$^{32}$P]-dCTP (Amersham BioSciences). X-ray films (AGFA) were exposed and then both the hybridized plasmid bands and the EtBr-stained chromosome were quantified using GelDoc (BioRad). *The amount of intracellular RepA in P. aeruginosa cells* carrying pPSEC plasmids was estimated by Western blotting, as described (47). 200 $\mu$l culture aliquots were taken at different $OD_{600}$ values. Total lysates were obtained, resolved by SDS-PAGE and transferred to nitrocellulose membranes by

electroblotting. Membranes were incubated with an anti-RepA rabbit polyclonal antiserum (1:1000) and then revealed with HRP-conjugated donkey anti-rabbit IgG (1:10000) by the ECL procedure (Amersham BioSciences). RepA amounts were estimated by comparing the intensities of the specific luminiscent bands in pPSEC-containing cells with those in lanes including extracts from plasmid free cells, the later supplemented with known amounts of pure RepA. The number of cells contributing to the loaded extracts was estimated after serial dilutions of the cultures, by counting at a microscope. Then viables were determined by plating on LB-agar supplemented with Kn. Molar concentration of RepA was calculated considering for a *P. aeruginosa* cell the same volume previously determined for *E. coli* ($4.6x10^{-10}$ $\mu$l) (48).

*EMSA*. DNA oligonucleotides containing either the operator or the four iteron sequences of pPS10 (18) were synthesized and then phosphorilated with T4 polynucleotide kinase. After annealing with their complementary strands, they were cloned into the *Sma*I site of pUC18 and sequenced. Plasmids were cut at the *Xba*I site and then labelled with 2 units of Klenow and 30 μCi of [α-$^{32}$P]-dCTP, for 30 min at 25 ºC. Fragments were excised with *Eco*RI and purified by electrophoresis in polyacrylamide gels (13). Increasing amounts of RepA proteins (WT or 2L2A) were incubated in ice with radiolabelled DNAs (4000 cpm) in 20 μl volume of 20 mM Hepes·$NH_4$ pH= 7.8, 5 mM β-MeEtOH, 0.1 mM EDTA, 6% glycerol, 50 $\mu$g/ml BSA. $(NH_4)_2SO_4$, provided by the supplied protein at 0.2 M. Samples, assembled in ice, were then transferred to room temperature for 30 minutes before loading into 6% polyacrylamide (29:1)-0.5xTBE gels. Electrophoresis was run at 150 V and 4 ºC. Gels were then dried-out and exposed to X-ray films.

*Analytical Ultracentrifugation*. *Sedimentation equilibrium* experiments were performed in a Beckman XL-A analytical ultracentrifuge. RepA stocks were dialyzed against 0.25 M $(NH_4)_2SO_4$, 50 mM $NH_4$-acetate pH= 6.0, 0.1 mM EDTA. 60 $\mu$l samples, with different

protein concentrations, were displayed into six channel centrifuge cells, with 1.2 cm optical path and centrepieces of epon charcoal. Sedimentation equilibrium gradients were formed at 5 ºC by spinning either at 13000 or 15000 rpm. Radial scans were taken at different wavelengths. Baseline offsets were measured at 50000 rpm. *Sedimentation velocity* of RepA, either alone or complexed with DNA fragments, was performed at 50000 rpm and 5 ºC with 350 $\mu$l samples displayed into double sector cells. Data from both types of experiments were processed as described (49). The sedimentation coefficient distributions for the RepA-DNA complexes (inset Fig. 6C) were calculated by direct linear least-squares boundary modelling of the sedimentation velocity data [ls-g*(s)] using SEDFIT (50).

*Spectroscopic Assays*. *Steady-State Fluorescence Spectroscopy* was performed in a Fluorolog Jobin Yvon-Spex spectrofluorimeter. 350 $\mu$l samples of His6-RepA-WT or His6-RepA-2L2A (5 $\mu$M) in 0.25 M $(NH_4)_2SO_4$, 50 mM $NH_4$-acetate pH= 6.0, 0.1 mM EDTA buffer were displayed into 0.2x1.0 cm path-length quartz cuvettes and left to equilibrate at 5 ºC. Trp94 in RepA was then selectively excited (2 nm slit) at 295 nm (21) and emission spectra were acquired between 300-450 nm (3 nm slit, $\Delta\lambda$= 1 nm). For extrinsic fluorescence measurements, bis-ANS (SIGMA) was supplied, from a stock in methanol, to a final concentration of 10 $\mu$M. Samples were left to equilibrate for 30 min at 5 ºC and then were excited at 395 nm. Emission spectra were acquired in the interval 400-600 nm. The contribution of the buffer was subtracted to all spectra. *Circular Dichroism Analysis* of His6-RepA-WT, His6-RepA-2L2A and their complexes with DNAs was performed in a Jasco-720 spectropolarimeter, using 0.1 cm path-length quartz cuvettes. The DNA oligonucleotides tested in the binding assays (RepA sites underlined) were:

1IR (operator): 5' GAACAA<u>GGACAGGG</u>CATTGACTTGT<u>CCCTGTCC</u>CTTAAT 3' (39-mer),

1DR (iteron): 5' ATACCC<u>GGGTTTAAAGGGGACAGATTCA</u>GGCTGTTATCCACACCC 3' (45-mer),

TEL (unrelated): 5' GATCCCACACCCACACACCCACACACCCACACACCCAG 3' (38-mer),

plus their complementary strands. Oligonucleotides were purified, and their concentrations determined, as described (21). Annealing was carried out by slow cooling in TE buffer and dsDNA stocks (50 $\mu$M) were stored at –20 ºC. Binding reactions (200 $\mu$l) were assembled in ice, in a solution containing 0.145 M $(NH_4)_2SO_4$, 50 mM $NH_4$-acetate pH= 6.0, 0.1 mM EDTA, 1 mM β-MeEtOH, 5% glycerol, plus 5 $\mu$M of protein and/or dsDNA. Spectra were acquired at 5 ºC from 320 to 200 nm, using a band width of 1 nm, 4 s response, 50 nm/min scan speed (0.2 nm steps) and 10 mdeg sensitivity. 5 to 10 spectra were accumulated for averaging. The spectrum of the buffer was subtracted and raw ellipticity data (in millidegrees) were transformed to molar ellipticity [θ] (in $deg.cm^2.dmol^{-1}$). No differences in the spectra were appreciated when reactions were incubated for variable times, ranging from 15 min to 3 h, indicating that binding equilibrium is reached rather quickly (42). Secondary structure estimates were performed with CDNN (51) at its web server (http://bioinformatik.biochemtech.uni-halle.de/cdnn/java/Started.html). Thermal denaturation analyses were performed on the same samples, overlaid with mineral oil. Ellipticity at 228 nm was measured meanwhile temperature of the cell holder was increased, using a computer-interfaced water bath, from 5 to 90 ºC (0.2 ºC steps, rate 20 ºC /hr, scans performed at 50 ºC /hr gave similar curves).

*Size Exclusion Chromatography*. Gel filtration assays were performed in a Superdex-200 HR10/30 column, assembled in an ÅKTA basic-10 HPLC equipment (Pharmacia). The column was equilibrated at room temperature in 0.145 M $(NH_4)_2SO_4$, 50 mM $NH_4$-acetate pH= 6.0, 0.1 mM EDTA, 1 mM β-MeEtOH, 5% glycerol. Duplicates (200 $\mu$l) of the samples previously assayed by CD spectroscopy (see above) were then injected. Chromatography was carried out at 0.5 ml/min in the same buffer, measuring the absorption of the eluate at 254 nm to optimize DNA detection.

**RESULTS**

*Rational Design and Functional Testing of a Monomeric RepA Mutant (RepA-2L2A).* We had previously described that point mutations, changing to Val the Leu residues of the N-terminal LZ-like sequence motif found in RepA, resulted in the displacement of dissociation equilibrium from dimers towards monomers when RepA was fused to MBP (14). This observation pointed to some (direct or indirect) role for the putative LZ in RepA dimerization. Such a hypothesis received additional support by the finding that an N-terminal deletion of the LZ-like motif (ΔN37) results in an increase in the monomeric fraction of that RepA fragment (21). However, we have since then noticed that: i) MBP-RepA fusions, albeit capable to bind the four iterons found in pPS10 origin of replication (14), have reduced binding cooperativity and fail to be wrapped by iteron DNA (not shown). ii) When expressed in the absence of the fusion with MBP, those RepA Leu --> Val mutants yielded unsoluble proteins, that we have been unable to refold *in vitro*. In order to clarify both the role of the LZ-like motif in RepA dimerization and the conformational change intrinsic to RepA monomerization (21) we have used the crystal structure of a monomeric homologous protein, RepE54 (24), to design RepA-2L2A. This is a new RepA mutant in which the first and second Leu residues of the hydrophobic LZ heptad (Leu12 and Leu19) have been substituted by Ala (Fig. 1). In RepE54 monomers, the LZ-like motif is found dislocated into two α-helices, resembling a folded *jack-knife*. The shortest one (α1) includes the first Leu residue (Leu12 in RepA) and the largest (α2) the third and fourth (Leu26 and Leu33), whereas the second (Leu19) is found in the intervening turn (Fig. 1B). The rationale behind the new Leu --> Ala mutations is as follows: i) They would impair a possible dimerization through the putative LZ, since the side chain of Ala is smaller and less hydrophobic than that of Leu. ii) They would necessarily disrupt the hydrophobic network linking α1, through Leu12 and Leu19, to the rest of the WH1 domain,

mainly Trp94. iii) Mutations would thus allow α1 to move freely, resulting in an extended conformation of the proposed *jack-knife*.

RepA-2L2A mutant was constructed by site-directed mutagenesis on an expression vector including *repA*-WT gene fused to His6 (21) (see Experimental Procedures). With the aim of testing the effect of the mutations on pPS10 replication *in vivo*, *repA*-2L2A was then transferred to a new pPS10-ColE1 shuttle vector (pPSEC1, Fig. 2A), replacing the parental *repA*-WT gene, to get pPSEC3. To check the effect of the His6 tag present in RepA-2L2A, a plasmid in which the *repA*-WT gene includes the sequence coding for the tag was also constructed (pPSEC2). After being rescued in *E. coli*, plasmids were transformed into *P. aeruginosa*. The transformation frequency of the *repA*-2L2A carrying plasmid decreased by three orders of magnitude when compared with those encoding for the WT proteins, whereas no differences were apparent between the tagged and untagged versions of RepA. After four rounds (≈ 80 generations) of replica plating with no selective pressure, the Kn resistance marker had been stably inherited in all clones. However, Southern blot analysis of total lysates from several Kn resistant pPSEC3 (*repA*-2L2A) colonies showed that the plasmid was integrated in the chromosome, instead of being replicated autonomously (not shown). This observation suggests that the mutant RepA-2L2A protein is inactive as DNA replication initiator. Growth curves for cells carrying plasmids encoding *repA*-WT show no significant differences between constructs with or without the His6 tag (Fig. 2B), confirming that the fused protein is fully functional as initiator. This was further proved by Southern blotting total lysates from mid-log phase cells, showing that there are no significant differences in plasmid copy number either (Fig. 2C). Western blot was performed, with anti-RepA polyclonal antiserum, on cells harvested at different stages of growth (Fig. 2B), showing similar protein levels for both versions of RepA-WT. Thus, besides to be active as initiator, His6-RepA is also able to regulate its own synthesis (Fig. 2D). Approximated quantification of the RepA

amounts yields about 860 protein molecules (or 430 dimers) per cell. This value is around the estimations for the Rep proteins of pSC101 (500 molecules) (41) and RK2 (300 molecules) (52) plasmids, but far from the those reported for R6K (about 20 fold higher) (53) and P1 (160 molecules) (47) initiators. It is relevant for the results presented later in this paper to note that pPS10 RepA is found at concentrations over 5 $\mu$M across all the growth curve (Fig. 2D).

EMSAs were performed to test if the failure of RepA-2L2A to act as initiator is due to have its DNA binding properties altered. Radiollabelled DNA fragments, including either *repA* operator sequence (Fig. 3A) or the four iterons found at pPS10 origin of replication (Fig. 3B), were incubated with increasing amounts of pure RepA protein, either WT (His6-tagged or untagged) or mutant 2L2A. The later was used with the His6 tag attached, since this increases its solubility and the tag, by itself, does not affect substantially DNA replication *in vivo* (Fig. 2, panels B and C). RepA-WT binding to operator DNA results in a typical pattern of two bands. These correspond to complexes including one or two protein dimers (D1 and D2, respectively, in Fig. 3A) (13,21), to finally yield large protein-DNA aggregates that remain in the well of the gel (W). However, only the first of such complexes, that with a single RepA dimer (D1), is observed with the 2L2A mutant. Its apparent dissociation constant ($Kd_{app}$, the protein concentration at which 50% of the DNA probe is bound) is at least 40 fold higher ($\geq$ 0.7 $\mu$M) than that for the His6 tagged RepA-WT (18 nM). Thus, although with a substantially decreased affinity, the RepA protein in which two Leu at its LZ-like motif (Leu12 and Leu19) were substituted by Ala seems able to dimerize upon binding to operator DNA. This observation points to the existence of an additional dimerization interface in RepA. It might most probably be the β-sheet in WH1, as proposed for RepE, based in the crystal structure of its monomer (24). Moreover, binding contacts of RepA-2L2A with the operator DNA must be unaffected, since they are made through WH2 (21) that it is intact in the mutant. The affinity of the tagged protein for the operator sequence appears to decrease:

about six-fold more His6-RepA-WT than RepA-WT is required to get a similar amount of bound DNA (Fig. 3A, lanes 1 and 3). In addition, the complex corresponding to the binding of a second RepA dimer (D2) does not appear. Thus since the *in vivo* data show that both versions (tagged and untagged) of RepA-WT are equally self-regulated (Fig. 2D), the formation of complex D2 seems not essential for *repA* promoter repression. D1 complexes, established by His6-RepA dimers, show a bit lower electrophoretic mobility than those for the untagged protein, probably due to the extra 4 kDa mass coming from the His6 tag. Concerning to the binding of RepA monomers to the iterons at the origin (Fig. 3B) (14), a sharp transition to large protein-DNA complexes, that remain in the well of the gel (W), is observed. This occurs even with the minimal amount of untagged RepA-WT tested (7.5 nM), whereas only a tiny fraction of DNA is found in discrete complexes (M1-M4). Although untagged RepA appears to bind cooperatively to iterons, its His6 version does not so much: DNA fragments with one to four iterons bound co-exist (M1-M4), and the complexes stacked in the well appear at higher protein concentration (≈ 50 nM). However, the observed differences in binding cooperativity between tagged and untagged RepA-WT have no significant effect on their function as DNA replication inititators *in vivo*, since the copy numbers of plasmids coding for them are very similar (Fig. 2C). On the contrary, RepA-2L2A fails to bind stably to iterons (M1 and M2 complexes appear at protein concentrations about 200-fold those operational with RepA-WT; not shown). This is not surprising since the domain altered in the mutant (WH1) was found in RepA-WT to bind the 5´ end of iteron sequence stably (21,24). The failure of RepA-2L2A to bind iterons *in vitro* is in accordance with the fact that the pPS10 derivative coding for this mutant (pPSEC3) can not be established autonomously *in vivo* (see above). Since the precise nature of the structural alteration induced by the mutations in RepA remained to be determined, we have performed a combined biophysical approach to further characterize the structure of RepA-2L2A.

*Physicochemical Characterization of RepA-2L2A as a Metastable Folding Intermediate.* One of the expected effects of the mutations designed in RepA-2L2A is to interfere with protein dimerization by altering the hydrophobic spine in the putative LZ α-helix (see above, Fig. 1B). In order to test the association state of RepA, we have performed sedimentation equilibrium experiments in an analytical ultracentrifuge. We have also addressed if the N-terminal His6 tag affects RepA-WT dimerization (Fig. 4, panels A and B), before determining the association state of RepA-2L2A (Fig. 4C). In this protein the His6 fusion was kept attached for improving solubility (see above). Ultracentrifugation runs were performed with a RepA range between the minimal concentration giving a reasonable signal to noise ratio with the absorption optics of the ultracentrifuge (1-2 $\mu$M) and a maximum close to the limits of RepA solubility (25 $\mu$M). RepA-WT remains essentially dimeric through all the concentration range tested (not shown), with a net tendency of the protein to assemble further, but no sign of dissociation. We had previously reported for a fusion with MBP that RepA-WT, in the lowest concentration range tested here, was close to the dissociation equilibrium between dimers and monomers (14). Now, in the light of our new data, that observed dissociation is revealed as a possible steric hindrance effect of the fused MBP moiety, probably caused by its large size (47 kDa). His6 tagged RepA-WT shows a similar behaviour to its untagged counterpart, with a slightly more marked tendency to associate beyond dimers (not shown). This is in accordance with data shown above pointing to similar *in vivo* and *in vitro* activities for both proteins (Figs. 2 and 3). Therefore, the rest of experiments described in this paper (Figs. 5-7) were carried out with the His6 tagged version of RepA-WT, to be compared straightforward with those performed with His6-RepA-2L2A. Sedimentation velocity analysis of His6 tagged and untagged RepA-WT, either at 5 or 15 $\mu$M, allowed to determine a sedimentation coefficient ($s_{20,w}$) for the RepA particle of 4.2 S and a frictional ratio ($f/f_o$) of 1.2 (not shown). These values are again compatible with being the most abundant RepA species dimers, with nearly

spherical shape. Thus it is relevant to underline that, based on the present analytical centrifugation analyses and at the conditions used in the spectroscopic studies described below, RepA-WT protein is largely found as stable dimers. Sedimentation equilibrium analysis on RepA-2L2A shows that this mutant protein is polydisperse: at the lower concentrations tested (2-7 $\mu$M), a significant monomeric fraction is found (Fig. 4C) together with large aggregates. These appear to become the major species at higher protein concentrations (not shown). Aggregation, previously described for deletion mutants affecting the putative LZ in RepA (21), can be attributed to the exposure of hydrophobic surfaces (probably an additional dimerization interface, see above) to the solvent. Both the disruption of RepA dimers and the exposure of hydrophobic residues, otherwise buried in the core of the folded N-terminal WH, were expected to arise from the double mutation designed in RepA-2L2A (Fig. 1B).

The possible structural changes induced by the 2L2A mutations were then explored by means of steady state fluorescence spectroscopy. Trp94, the single tryptophan residue in RepA (18,21), is a key node in the network attaching Leu12 and Leu19 to the hydrophobic core of WH1 (Fig. 1B). Thus, it is expected to be a suitable spectroscopic sensor for any structural modification in its environment. RepA-WT has nine tyrosines (18). Comparing the excitation and emission spectra of RepA with those for free tyrosine and N-acetyl-tryptophanamide solutions we have verified that, at 295 nm, no Tyr residue is excited in RepA. On the contrary, that wavelength falls in the tail of the excitation spectrum of Trp94 (not shown). Thus, Trp94, either in RepA-WT or in RepA-2L2A (5 $\mu$M), was selectively excited at 295 nm and then fluorescence emission spectra were acquired (Fig. 5A). The maximum emission was achieved at 327 nm (RepA-WT) or 348 nm (RepA-2L2A). The extra band at 335 nm observed in RepA-2L2A emission suggests the presence of two major populations of different rotamers for Trp94 side chain. The red-shifted emission found for

RepA-2L2A is characteristic of exposed Trp residues and it is compatible with the increased solvent accessibility expected for Trp94 after the release of its hydrophobic linkage to the bipartite α-helix (Fig. 1B). On the contrary, the emission of Trp94 in RepA-WT, close to 320 nm, is typical of Trp residues buried in a protein core, or in a contacting interface (21). The wavelength for the emission maximum in RepA-WT did not change after serial dilutions of the protein sample (tested up to 78 nM, not shown), providing further evidence for its dimeric association state in a broad concentration range. Another clue for a structural change affecting Trp94 in RepA-2L2A is its enhanced fluorescence emission intensity compared with that for the WT protein (Fig. 5A). To get additional proof for the presence of exposed hydrophobic residues in RepA-2L2A, an extrinsic fluorescence probe was used: bis-ANS, a naphtalene derivative that binds to solvent accessible hydrophobic patches in proteins, enhancing its fluorescence emission over 450 nm (21). Incubation of bis-ANS (10 $\mu$M) with RepA-WT or 2L2A (5 $\mu$M) results in spectra with emission maxima around 472 nm (Fig. 5B). The fluorescence intensity at this wavelength is 61% higher for Rep-2L2A than for the WT protein, confirming that the former has a larger hydrophobic surface exposed to the solvent.

As a summary of the results shown so far, RepA-WT is a stable dimer *in vitro* in a broad ($\mu$M) concentration range (Fig. 4A), similar to that found in *P. aeruginosa* cells (Fig. 2D). In terms of RepA association state (Fig. 4B), DNA binding properties (Fig. 3) or even its activity as a DNA replication initiator *in vivo* (Fig. 2), there is no significant difference in having a His6 peptide fused to RepA N-terminus. RepA-2L2A, in which two Leu residues in the putative LZ (Leu12 and Leu19) were substituted by Ala (Fig. 1), exposes hydrophobic residues to the solvent, as revealed by fluorescence studies (Fig. 5) and by its enhanced tendency to aggregation. Thus, it exhibits the biophysical properties expected for a metastable monomeric (Fig. 4C) protein folding intermediate (54).

*Binding to Iteron DNA Dissociates RepA Dimers into Monomers and Acts as Allosteric Effector on Protein Conformation*. With the aim of deepen our understanding on the structural basis of the recognition of operator and iteron DNA sequences by RepA dimers and monomers, respectively, we have performed a CD spectroscopy study on RepA-DNA complexes (Figs. 6 and 7). 5 $\mu$M of His6 tagged RepA-WT protein were incubated with equimolar amounts of double-stranded oligonucleotides, including either the *repA* operator sequence (1IR), a single iteron (1DR) or an unrelated sequence of similar size (yeast telomeric TEL). Fig. 6A shows overlaid the CD spectra of the oligonucleotides alone and in complex with RepA-WT. The bands with positive ellipticity (θ) in the near U.V. range of the spectra (320-250 nm) arise from the stacking of DNA bases, with nearly null contribution from protein aromatic residues. In the far U.V. (250-200 nm) the predominant contribution comes from the protein moiety. Having no substantial differences in the spectra, between 320 and 250 nm, for the free and protein-bound states of a given DNA can be interpreted as a sign of no significant structural alterations in the DNA (55). Since that is the case for the distinct RepA-DNA complexes in Fig. 6A, the spectra of free DNAs can be subtracted from those of their complexes with RepA, thus focusing in possible structural changes on the protein side. The result of this algebraic operation is depicted in Fig. 6B, in which two types of protein spectra become evident: i) Curves with double minima at about 208 and 222 nm, a signature for a significant proportion of α-helical secondary structure (33%). These correspond to free RepA-WT and in complex with the operator oligonucleotide 1IR. ii) Curves with a broader minimum around 215 nm, attributable to an increase in the β-sheet component (by about 4%) at the expense of former α-helices, as observed for RepA-WT in complex with the iteron oligonucleotide 1DR. It is relevant that RepA-WT does not change its spectrum, and thus its structure to a detectable extend, when it is free in solution or bound to the operator. This is coincident with the fact that RepA is essentially an homogeneous dimer in solution at this

concentration (Fig. 4B) and that it binds to that DNA sequence as a dimer (Fig. 3A) (14). However, when it binds to the iteron DNA as a monomer (Fig. 3B) (14) its spectrum resembles that of the mostly monomeric RepA-2L2A mutant (Fig. 6B). We have failed to acquire clean spectra for complexes between this mutant protein and any DNA, since a cloudy precipitate appears. Although less severe, protein aggregation is also observed, in the form of noisy spectra, for the non-specific complexes between RepA-WT and DNAs of unrelated sequence, such as TEL (Fig. 6), other mixed sequence oligonucleotides and poly-(dI-dC) (data not shown). As a summary, our spectroscopic studies show that RepA has a distinct secondary structure composition when bound to the inversely-repeated operator sequence or to the directly-repeated iteron DNA.

In order to correlate the observed conformational change with the association state of RepA, we carried out EMSAs (not shown), size exclusion chromatography (Fig. 6C) and sedimentation velocity (inset Fig. 6C) on the same samples tested by CD. EMSAs consistently result in that the RepA-operator complex slightly has lower electrophoretic mobility than the RepA-iteron band (not shown). Taking into account that the free iteron oligonucleotide (1DR) is 6 bp larger than the operator one (1IR), this result is compatible with having a larger protein mass in the later complex (a dimer) than in the former (a monomer). However, EMSAs are not conclusive since the minute difference in the electrophoretic migration between both types of complexes could be also due to disparate bending behaviour of the bound DNA fragments. For the sample including RepA and the unrelated oligonucleotide TEL, no discrete retarded band is visible but some smearing indicative of low affinity, non-specific, binding (not shown). When the samples were injected into a size exclusion column the specific RepA-oligonucleotide complexes remain stable and their hydrodynamic behaviour (Fig. 6C) was unambiguous. The relative elution position of the peaks corresponding to bound DNAs is reverse to that for the unbound species (the assay is sensitive enough to detect the

aforementioned slight difference in the sizes of free oligonucleotides). This fact can be explained if the protein mass associated with the smaller operator DNA piece (1IR) is substantially larger (a dimer) than that associated with the longer iteron (1DR) fragment (a monomer). The possibility of having just one subunit in a RepA dimer bound to the iteron, as proposed for the Rep protein of R6K plasmid (16), is thus very unlikely. Such a complex would be expected to elute just before the RepA-operator one. In order to characterize further the nature of the complexes eluted from the gel filtration column, analytical ultracentrifugation was performed. Unfortunately, RepA-DNA complexes dissociate during the time course required to achieve sedimentation equilibrium (not shown). However, the interpretation proposed above is in agreement with the results of sedimentation velocity experiments performed, immediately after the gel filtration runs, with the peak fractions. There is a substantial difference in the sedimentation coefficients for the RepA-1IR (6.5 ± 0.2 S) and the RepA-1DR (3.8 ± 0.2 S) complexes. These sedimentation coefficients are only compatible with being the RepA-1IR complex significantly more compact ($f/f_o$ =1.2) than RepA-1DR ($f/f_o$ =2.0). The later value fits with the elongated shape of a complex between a RepA monomer and an oligonucleotide with identical length than 1DR, modelled on the crystal structure of RepE54 (24) (not shown). Therefore, our results clearly show that the structural changes in RepA coupled with binding to iteron DNA (Fig. 6B) are linked to dissociation of the otherwise stable protein dimers (Fig. 4B) into monomers (Fig. 6C).

It is noteworthy that, for unbound RepA, we have not found any sign of dissociation of dimers after incubation times ranging from 30 min (spectroscopy, Figs. 5 and 6) to 16 hrs (sedimentation equilibrium, Fig. 4). On the contrary, upon incubation with origin DNA RepA dissociation (Fig. 6C) and the coupled structural transformation (Fig. 6B) occur within a few minutes. Since serial dilutions of unbound RepA exhibit the fluorescence emission spectrum characteristic of dimers (Fig. 5A) at least up to low nanomolar concentrations (not shown), the

possibility that at 5 $\mu$M a small fraction of monomeric RepA, in equilibrium with dimers, would bind to the iteron sequence and that this event would drive monomer formation seems unlikely. In summary, there are solid basis to affirm that: i) Since the Kd for RepA dimers appears to be in the low nanomolar-subnamolar range, in our experimental (micromolar) conditions the equilibrium is well displaced towards the dimeric species. ii) Along broad time courses no monomeric unbound fraction has been detected for RepA. Thus the reported induction of RepA dissociation by iteron DNA seems to be genuine.

Thermal denaturation analyses performed by optical techniques, such as CD spectroscopy, provide valuable information on the thermodynamic stability of proteins (4,21) and their complexes with DNA (55). We have carried out this kind of approach to study the effect on RepA stability of binding to the DNA sequences described above (Fig. 6). Inspection of the CD spectra in Fig. 6A reveals that, at 228 nm, the contribution of the oligonucleotides to the ellipticity ($\theta$) of their complexes with RepA is essentially null, whereas that from the $\alpha$-helical and $\beta$-sheet structural elements in RepA (Fig. 6B) is significant. Thus, we plotted the variation of $\theta_{228}$ with temperature for each kind of RepA-DNA complex (Fig. 7) and then compared the resulting curves. Since thermal denaturation of RepA and its complexes is irreversible, a detailed thermodynamic analysis of the CD profiles was precluded. The temperature at which 50% of protein molecules unfold (Tm) was determined, because it is essentially unaffected by irreversibility and gives an idea on protein stability. Binding to operator DNA (1IR) stabilizes RepA, relative to its unbound state, by 12.4 ºC, whereas binding to iteron DNA has a smaller effect (4.8 ºC). The more pronounced slope of the curve for 1IR complexes indicates that RepA denaturation becomes more cooperative upon operator binding by the dimers. This effect is also observed for the complexes of RepA monomers with iteron DNA (1DR), although to a less extend. However, binding to non-specific sequences (TEL) severely decreases the stability of RepA (by 11.5 ºC), approaching the Tm values

measured for the mostly monomeric folding intermediate RepA-2L2A (Fig. 7) and for a previously reported N-terminal partial deletion derivative (ΔN37) (21). This observation suggests that, as reported for some restriction endonucleases (56), non-specific DNA could, to some extend, exert conformational changes in RepA (Fig. 6B) enabling it to scan for specific iteron sequences. However, the resulting RepA molecules seem to be unstable folding intermediates that, due to the exposure of hydrophobic residues prone to aggregation (see above), would recruit molecular chaperones. Therefore, iteron DNA not only acts as allosteric conformational effector on RepA dimers (Fig. 6B), but also has a role in stabilizing the structure of the resulting monomers.

## DISCUSSION

*RepA-2L2A: a Folding Intermediate in the Pathway from Repressor Dimers to Initiator Monomers*. In this paper we have described the design of RepA-2L2A, a mutant in the protein that initiates DNA replication of the *Pseudomonas* plasmid pPS10, based on the available three-dimensional structure of the monomer of a homologous initiator (24). RepA-2L2A carries a double Leu --> Ala substitution (Leu12 and Leu19) in the LZ-like motif found in the protein (14,19,21). These mutations were expected to enhance dissociation of an otherwise dimeric protein into monomers, and to destabilize the hydrophobic core of the later (Fig. 1). Functional characterization of RepA-2L2A indicates that it is inactive as initiator of replication (Fig. 2). RepA-2L2A has affected its binding to iteron DNA sequences (Fig. 3B) and reduced its affinity for operator DNA (Fig. 3A), where RepA binds as a dimer (13,21). Hydrodynamic studies (Fig. 4) show that RepA-2L2A can be largely found as a monomer in a narrow micromolar range, forming non-specific aggregates at higher concentrations. Dimerization of WH domains (23) through hydrophobic residues in the α-helices equivalent to α2 and α4 in Rep proteins (Fig. 1) has been described for the complex between the eukaryotic

transcription factors E2F4 and DP2 (57). However, a role in dimerization for the antiparallel β-sheet found at the N-terminal WH domain of RepE54 is also possible (24). To determine if the LZ-like motif has a direct contribution to the interprotomeric contacts in RepA dimers, or if it rather favours RepA association indirectly (e.g.: stabilizing the dimeric conformation) will require to solve the three-dimensional structure of a Rep protein dimer. Spectroscopic evidence (Fig. 5) supports that RepA-2L2A resembles a transient folding intermediate, with hydrophobic residues partially exposed to the solvent, expected to occur in the pathway from repressor dimers to initiator monomers. This is the first report on the isolation and characterization of a conformational intermediate in a Rep-type initiator protein. In addition, we have shown that short His6 fusions to RepA have a minor effect on the association state of the protein *in vitro* (Fig. 4B), that remains as a dimer in a broad micromolar range. The His6-tag does not alter RepA initiator activity *in vivo* (Fig. 2), in spite of showing some reduction in its binding cooperativity to iteron sequences *in vitro* (Fig. 3B).

*The Allosteric Effect of Iteron Binding on RepA Conformation and Association State*. At the same concentration in which RepA is a dimer (Fig. 4) with no sign of dissociation into monomers, binding to an oligonucleotide encoding for a single iteron origin sequence results in: i) Dissociation of RepA into monomers (Fig. 6C). ii) A change in protein secondary structure, which becomes similar to that for the monomeric intermediate RepA-2L2A (Fig. 6B). On the contrary, the structure of RepA dimers appears to be unaltered by binding to the inversely-repeated operator sequence (Fig. 6B). Interestingly, binding to both types of DNA stabilizes RepA against thermal denaturation, although to a different extend (Fig. 7). This fact also points to differences in the structures of RepA dimers and monomers. In the same experimental conditions, non-specific DNA oligonucleotides result in precipitation of RepA and in destabilization of the structure of the protein (Fig. 7). Structural changes in a number of DNA binding proteins upon specific ligand recognition have been previously reported as cases

of allosterism (44,45,56). However, apart from being found in some viral initiators (58,59) and in ORC with single-stranded DNA (5), they are new events in the initiation of DNA replication in bacterial plasmids.

The precise mechanism through which iteron DNA exerts the allosteric effect on RepA structure described in this paper remains to be determined in its molecular details. It is worth noting that in the eukaryotic transcription factor Ets1 an α-helix (αI-2) is found at the N-terminus of the three α-helices of its WH domain (60), packing against the first helix very much as α1 and α2 do in Rep proteins (Fig. 1B). A phosphate in DNA backbone triggers an allosteric transition in Ets1 αI-2 by establishing a hydrogen bond with the amide NH of a Leu residue at α1 N-terminus. This corresponds in RepE54 monomers with Arg33 (Fig. 1B), which also binds to iteron phosphate backbone in the crystal structure (24), whereas modelling of Rep dimers suggests that it must be displaced apart from the operator phosphate backbone (24). Arg33 in RepE54 consistently aligns with hydrophobic residues (mainly Leu, as in Ets1) in RepA, other members of its family (9,10,24) and the eukaryotic and archaeal initiators Orc4/Cdc6 (4). Thus a way is opened to a possible general role of this residue in triggering allosteric transitions in WH initiator proteins.

*On the Role of Chaperones and Specific Origin Sequences in the Structural Activation of Rep Proteins*. At the concentrations it is found in *Pseudomonas* cells *in vivo* (Fig. 2D), RepA is dimeric (Fig. 4), acting as transcriptional repressor (13,20). It has been found for P1 (34,42) and pSC101 (41) plasmids that their Rep proteins can spontaneously dissociate into monomers just by dilution to low/sub-micromolar concentration. However, besides pPS10 RepA, the initiators of F (12), R6K (16,61) and RK2 (15,36) plasmids have their Kds in the low nanomolar range. For the later the requirement for an active mechanism in Rep dissociation, and in the coupled conformational change, thus remains as a bottleneck. Our findings on the ability of an iteron sequence to induce structural transitions in RepA confer a

property to origin DNA that was previously attributed to chaperone action alone (reviewed in 30).

Based on data presented in this paper, we propose that the structural changes in Rep that are coupled to dimer dissociation would imply: i) Releasing protein-protein interactions between protomers, involving the LZ-like motif and/or the β-sheet in the first domain (21,24). ii) Remodelling the hydrophobic core of WH1, where the relevant Leu residues (Leu12 and Leu19) are tightly packed with Trp94 (Fig. 1B). iii) An increase in β-strand structure at the expense of the α-helical components (Fig. 6B). The rearrangement experienced by Rep would necessarily generate transient intermediates with properties similar to those of the RepA-2L2A mutant, namely having hydrophobic sequence patches exposed to the solvent and a loosely folded core (Fig. 5), both features of "molten globules" (54). This explains why monomeric RepA, when free in solution and in the absence of iteron DNA, is prone to aggregation through WH1 (see above) (21). In order to cope with these challenges to Rep activation, different, albeit complementary, molecular mechanisms can be envisaged.

Chaperones can directly dissociate Rep dimers, and simultaneously change the conformation of the monomers, in order to make them competent for iteron binding. This has been reported for the DnaK-DnaJ-GrpE triad (11,31,33-35), ClpA (32,43) and ClpX (36). These could target WH1 in Rep: ClpA recognizes a region at the N-terminus of P1 Rep (residues 10-70) (62) as the first step towards unfolding, either for its activation as initiator or for degradation by the associated ClpP protease (37,38). DnaK, on its side, recognizes a hydrophobic patch (residues 36-49) in the same Rep protein (63), which in pPS10 RepA corresponds to a sequence (residues 91-105) comprising the Trp94 residue discussed above. We had previously shown that pPS10 replication *in vitro* is sensible to DnaK levels (64). Although they physically interact (4), if DnaK is acting on RepA dissociation remains to be determined. For those Rep dimers that dissociate spontaneously, chaperones could bind to

exposed hydrophobic regions (65) in the monomeric intermediates, thus protecting them from falling into local energy minima that would act as kinetic traps in the pathway leading to Rep folding and iteron binding. Otherwise, large Rep aggregates could arise from the accumulation of monomeric intermediates but it seems feasible that the combined action of several chaperones, such as ClpB plus DnaK-DnaJ-GrpE (66), could rejuvenate them into active initiators.

The allosteric conformational changes induced in RepA by iteron DNA (Fig. 6) would constitute another means to get the monomeric species, specially for those Rep proteins that are stable dimers at the concentrations they are found *in vivo* (Fig. 2D) (16,52,53). This way could be favoured by the cooperativity of Rep binding to DNA (Fig. 3B). Alternatively, iteron DNA could also capture and stabilize the monomeric folding intermediates produced after spontaneous dissociation of Rep dimers, as proposed above for chaperones. An implication of this new activation mechanism is that only a fraction of the total amount of Rep molecules, coincident with the number of iteron sequences, would be eventually activated while the others would remain dimeric. On the contrary, there is no obvious means to limit the number of active Rep monomers generated by the chaperone-mediated route, that could be accumulated in excess over the levels required for regulated initiation. In addition, the allosteric binding of iteron DNA to RepA implies that the structural changes associated to monomerization are intrinsically accessible to Rep proteins, and not necessarily the exclusive product of chaperone action.

In plasmids containing iteron sequences at their origins of replication, the most favoured model for negative control of initiation implies pairing distant Rep-bound iteron repeats ("handcuffing") (30,67). Except in R6K plasmid (16) handcuffing appears to be mediated by Rep monomers. However, in some Rep proteins, a number of mutants have been isolated that being monomeric hyperactive initiators, fail to pair iterons (40,68). Most of such mutations

fall in a putative additional dimerization interface in Rep that, besides the LZ-like motif, we have discussed for RepA-2L2A. Thus, Rep proteins activated by the allosteric route resemble the behaviour of those hyperactive mutants. The minimal requirements for pairing are two DNA fragments containing each a single iteron repeat (69), but we have failed to detect handcuffing even at 5 $\mu$M RepA-iteron complex concentration (Fig. 6C). Our model leaves open the possibility for the existence of two kinds of Rep monomers, correlated with their opposite functions as initiators or negative regulators of plasmid DNA replication. Thus, unwinding of origin DNA after the formation of the Rep-iteron nucleoprotein complex might induce a further conformational change in the monomers, as described for the chromosomal initiators ORC in eukaryotes (5) and DnaA in bacteria (6). RepA would then become competent for origin pairing, but disabled for a new round of initiation on recently replicated DNA.

**ACKNOWLEDGEMENTS**

We are indebted to all other members of our lab, past and present, for their support in our research on RepA, specially to Dr. D. García de Viedma for the kind gift of anti-RepA serum. We are grateful to the staff members of the oligonucleotide synthesis and DNA sequencing facilities at CIB for their excellent technical support. Thanks are also due to Dr. P. Lillo for the critical reading of the manuscript. This work was supported by grants of the Spanish CICYT (PM99-0096) and Red Temática de Investigación Cooperativa (FIS C03/14).

**REFERENCES**

1. Kornberg, A. and Baker, T. (1992) *DNA replication*, 2nd ed., W.H.Freeman, New York.

2. Baker, T. A. and Bell, S. P. (1998) *Cell*, **92**, 295-305.

3. Lee, D. G. and Bell, S. P. (2000) *Curr. Op. Cell Biol.* **12**, 280-285.

4. Giraldo, R. and Díaz-Orejas, R. (2001) *Proc. Natl. Acad. Sci. USA*, **98**, 4938-4943.

5. Lee, D. G., Makhov, A. M., Klemm, R. D., Griffith, J. D. and Bell, S. P. (2000) *EMBO J.* **19**, 4774-4782.

6. Speck, C. and Messer, W. (2001) *EMBO J.* **20**, 1469-1476.

7. Messer, W. (2002) *FEMS Microbiol. Rev.* **26**, 355-374.

8. Klemm, R.D., Austin, R. J. and Bell, S. P. (1997) *Cell*, **88**, 493-502.

9. del Solar, G., Giraldo, R., Ruíz-Echevarría, M. J., Espinosa, M. and Díaz, R. (1998) *Microbiol. Mol. Biol. Rev.* **62**, 434-464.

10. Cohen, S., Couturier, M, del Solar, G., Díaz-Orejas, R., Espinosa, M., Giraldo, R., Jánniere, L., Miller, C., Osborn, M. and Thomas, C. M. (2000) In *The Horizontal Gene Pool: Bacterial plasmids and gene spread* (Thomas, C. M., ed), pp. 1-47, Harwood Academic Publishers, UK.

11. Wickner, S., Hoskins, J. and McKenney, K. (1991) *Proc. Natl. Acad. Sci. USA*, **88**, 7903-7907.

12. Ishiai, M., Wada, C., Kawasaki, Y. and Yura, T. (1994) *Proc. Natl. Acad. Sci. USA*, **91**, 3839-3843.

13. García de Viedma, D., Giraldo, R., Ruíz-Echevarría, M. J., Lurz, R. and Díaz-Orejas, R. (1995) *J. Mol. Biol.* **247**, 211-223.

14. García de Viedma, D., Giraldo, R., Rivas, G., Fernández-Tresguerres, E. and Díaz-Orejas, R. (1996) *EMBO J.* **15**, 925-934.

15. Toukdarian, A., Helinski, D. R. and Perri, S. (1996) *J. Biol. Chem.* **271**, 7072-7078.

16. Urh, M., Wu, J., Wu, J., Forest, K., Inman, R. B. and Filutowicz, M. (1998) *J. Mol. Biol.* **283**, 619-631.

17. Krüger, R., Konieczny, I. and Filutowicz, M. (2001) *J. Mol. Biol.* **306**, 945-955.

18. Nieto, C., Giraldo, R., Fernández-Tresguerres, E. and Díaz, R. (1992) *J. Mol. Biol.* **223**, 415-426.

19. Giraldo, R., Nieto, C., Fernández-Tresguerres, M. E. and Díaz, R. (1989) *Nature*, **342**, 866.

20. García de Viedma, D., Serrano-López, A. and Díaz-Orejas, R. (1995) *Nucl. Acids Res.* **23**, 5048-5054.

21. Giraldo, R., Andreu, J. M. and Díaz-Orejas, R. (1998) *EMBO J.* **17**, 4511-4526.

22. Gajiwala, K. S. and Burley, S. K. (2000) *Curr. Op. Struct. Biol.* **10**, 110-116.

23. Liu, J., Smith, C. L., DeRyckere, D., DeAngelis, K., Martin, G. S. and Berger, J. M. (2000) *Mol. Cell*, **6**, 637-648.

24. Komori, H., Matsunaga, F., Higuchi, Y., Ishiai, M., Wada, C. and Miki, K. (1999) *EMBO J.* **18**, 4597-4607.

25. Kawasaki, Y., Matsunaga, F., Kano, Y., Yura, T. and Wada, C. (1996) *Mol. Gen. Genet.* **253**, 42-49.

26. Konieczny, I., Doran, K. S., Helinski, D. R. and Blasina, A. (1997) *J. Biol. Chem.* **272**, 20173-20178.

27. Park, K., Mukhopadhyay, S. and Chattoraj, D. K. (1998) *J. Biol. Chem.* **273**, 24906-24911.

28. Sharma, R., Kachroo, A. and Bastia, D. (2001) *EMBO J.* **20**, 4577-4587.

29. Pacek, M., Konopa, G. and Konieczny, I. (2001) *J. Biol. Chem.* **276**, 23639-23644.

30. Chattoraj, D. K. (2000) *Mol. Microbiol.* **37**, 467-476.

31. Wickner, S., Skowyra, D., Hoskins, J. and McKenney, K. (1992) *Proc. Natl. Acad. Sci. USA*, **89**, 10345-10349.

32. Wickner, S., Gottesman, S., Skowyra, D. F., Hoskins, J., McKenney, K. and Maurizi, M. R. (1994) *Proc. Natl. Acad. Sci. USA*, **91**, 12218-12222.

33. Sozhamannan, S. and Chattoraj, D. K. (1993) *J. Bacteriol*. **175**, 3546-3555.

34. DasGupta, S., Mukhopadhyay, G., Papp, P. P., Lewis, M. S. and Chattoraj, D. K. (1993) *J. Mol. Biol*. **232**, 23-34.

35. Kawasaki, Y., Wada, C. and Yura, T. (1990) *Mol. Gen. Genet*. **220**, 277-282.

36. Konieczny, I. and Helinski, D. R. (1997) *Proc. Natl. Acad. Sci. USA*, **94**, 14378-14382.

37. Hoskins, J. R., Singh, S. K., Maurizi, M. R. and Wickner, S. (2000) *Proc. Natl. Acad. Sci. USA*, **97**, 8892-8897.

38. Ishikawa, T., Beuron, F., Kessel, M., Wickner, S., Maurizi, M. R. and Steven, A. C. (2001) *Proc. Natl. Acad. Sci. USA*, **98**, 4328-4333.

39. Dibbens, J. A., Muraiso, K. and Chattoraj, D. K. (1997) *Mol. Microbiol*. **26**, 185-195.

40. Mukhopadhyay, G, Sozhamannan, S. and Chattoraj, D. K. (1994) *EMBO J*. **13**, 2089-2096.

41. Ingmer, H., Fong, E. L. and Cohen, S. (1995) *J. Mol. Biol*. **250**, 309-314.

42. Chattoraj, D. K., Ghirlando, R., Park, K., Dibbens, J. A. and Lewis, M. S. (1996) *Genes to Cells*, **1**, 189-199.

43. Pak, M. and Wickner, S. (1997) *Proc. Natl. Acad. Sci. USA*, **94**, 4901-4906.

44. Spolar, R. S. and Record, T. M. Jr. (1994) *Science*, **263**, 777-784.

45. Jen-Jacobson, L., Engler, L. E. and Jacobson, L. A. (2000) *Structure*, **8**, 1015-1023.

46. Fernández-Tresguerres, M. E., Martín, M., García de Viedma, D., Giraldo, R. and Díaz-Orejas, R. (1995) *J. Bacteriol*. **177**, 4377-4384.

47. Swack, J. A., Pal, S. K., Mason, R. J., Abeles, A. L. and Chattoraj, D. K. (1987) *J. Bacteriol*. **169**, 3737-3742.

48. Brenner, M. and Tomizawa, J.-I. (1991) *Proc. Natl. Acad. Sci. USA,* **88**, 405-409.

49. Abril, A. M., Salas, M., Andreu, J. M., Hermoso, J. M. and Rivas, G. (1997) *Biochemistry*, **6**, 11901-11908.

50. Schuck, P. and Rossmanith, P. (2000) *Biopolymers* **54**, 328-341.

51. Bohm, G., Muhr, R. and Jaenicke, R. (1992) *Prot. Eng.* **5**, 191-195.

52. Durland, R. H. and Helinski, D. R. (1990) *J. Bacteriol.* **172**, 3849-3858.

53. Filutowicz, M., McEachern, M. J. and Helinski, D. R. (1986) *Proc. Natl. Acad. Sci. USA*, **83**, 9645-9649.

54. Ptitsyn, O. B. (1995) *Adv. Prot. Chem.* **47**, 83-229.

55. Dao-Thi, M.-H., Messens, J., Wyns, L. and Backmann, J. (2000) *J. Mol. Biol.* **299**, 1373-1386.

56. Viadiu, H. and Aggarwal, A. K. (2000) *Mol. Cell*, **5**, 889-895.

57. Zheng, N., Fraenkel, E., Pabo, C. O. and Pavletich, N. P. (1999) *Genes Dev.* **13**, 666-674.

58. Lima, L. M. T. R. and de Prat-Gay, G. (1997) *J. Biol. Chem.* **272**, 19295-19303.

59. Cruickshank, J., Shire, K., Davidson, A. R., Edwards, A. M. and Frappier, L. (2000) *J. Biol. Chem.* **275**, 22273-22277.

60. Wang, H., McIntosh, L. P. and Graves, B. J. (2002) *J. Biol. Chem.* **277**, 2225-2233.

61. Wu, J., Sektas, M., Chen, D. and Filutowicz, M. (1997) *Proc. Natl. Acad. Sci. USA*, **94**, 13967-13972.

62. Hoskins, J. R., Kim, S.-Y. and Wickner, S. (2000) *J. Biol. Chem.* **275**, 35361-35367.

63. Kim, S.-Y., Sharma, S., Hoskins, J. R. and Wickner, S. (2002) *J. Biol. Chem.* **277**, 44778-44783.

64. Giraldo, R., Martín, M., Fernández-Tresguerres, M. E., Nieto, C. and Díaz, R. (1992) In *DNA replication: The regulatory mechanisms* (Hughes, P., Fanning, E and Kohiyama, M., eds.), pp. 225-237, Springer Verlag, Berlin.

65. Bukau, B. and Horwich, A. L. (1998) *Cell*, **92**, 351-366.

66. Goloubinoff, P., Mogk, A., Ben-Zvi, A. P., Tomoyasu, T. and Bukau, B. (1999) *Proc. Natl. Acad. Sci. USA*, **96**, 13732-13737.

67. Park, K., Han, E., Paulsson, J. and Chattoraj, D. K. (2001) *EMBO J*. **20**, 7323-7332.

68. Blasina, A., Kittell, B. L., Toukdarian, A. E. and Helinski, D. R. (1996) *Proc*. *Natl*. *Acad*. *Sci*. *USA*, **93**, 3559-3564.

69. Papp, P. P, Mukhopadhyay, G. and Chattoraj, D. K. (1994) *J*. *Biol*. *Chem*. **269**, 23563-23568.

**LEGENDS TO FIGURES**

Fig. 1. **A structural framework for the design of RepA mutants affected in dimerization and conformational activation**. ***A***, Overview of the WH1 domain of the monomeric RepE54 initiator from mini-F plasmid (PDB entry 1REP) (24), with its α-helical elements highlighted in red: α3 and α4 constitute the HTH motif, in which the later is the DNA recognition helix. ***B***, Slab view removing the HTH to uncover α1 and α2, that include Leu residues conforming to a LZ-like sequence motif (19). The first two of such leucines (Leu12 and Leu19), substituted by Ala to generate the RepA-2L2A mutant, are depicted in green. In cyan is the single Trp in RepA (Trp94) that is a crucial part of the network of hydrophobic interactions (distances displayed in white) to which Leu12 and Leu19 also contribute. These three residues, absolutely conserved in RepA, RepE54 and other Rep proteins (9,10,24), are numbered according to RepA sequence, but the others (in orange) keep the original labelling from RepE54 (24). A dashed purple arrow indicates the expected *jack-knife* movement that would undergo the N-terminal α1 helix around the hinge including Leu19, once the hydrophobic network is disrupted by the mutations in RepA-2L2A that, in addition, would hamper any possible dimerization through the leucines.

Fig. 2. **Testing the functionality of RepA-2L2A and the effect of the N-terminal His6 tag *in vivo***. ***A***, Scheme of the shuttle plasmid series pPSEC, including a ColE1 type replicon, for maintenance in *E. coli*, and the pPS10 replicon, for propagation in *Pseudomonas*. The pPS10 origin of replication (*oriV*) and sequences 5´ to the *repA* gene are enlarged to highlight the differences between plasmids: Having His6 tags encoded in *repA* (pPSEC2/3) or not (pPSEC1), and including the *repA*-2L2A mutation (pPSEC3) or not (pPSEC1/2). All the clones transformed with pPSEC3 were found to have this plasmid integrated in the chromosome (not shown), and thus are not included in subsequent panels. ***B***, Growth curves

for *P. aeruginosa* cells carrying the plasmids pPSEC1 or pPSEC2. ***C***, Southern blotting of total lysates from mid-log *P. aeruginosa* cells, carrying the plasmids pPSEC1 or pPSEC2. Upper panel shows the chromosome bands stained with EtBr, whereas the lower part corresponds to the signal of $^{32}$P-labelled *repA* gene hybridized with the plasmids. The relative plasmid copy number is indicated below each track, corrected for loading bias by chromosome density and normalized to the value of pPSEC1. ***D***, Western blotting, with polyclonal anti-RepA serum, of total cell extracts obtained at different points of the growth curve in B. First two tracks: Purified RepA standards loaded together with a total lysate from plasmid-free *P. aeruginosa* cells. The estimated amount of RepA, the number of cells contributing to the load and the concentration of RepA in the cells are indicated below each track.

Fig. 3. **EMSA on the complexes established by RepA, and its His6 and 2L2A variants, at the operator and origin sequences**. ***A***, Titration of a $^{32}$P-labelled DNA fragment (0.17 nM) including the operator inverted repeat. F: Unbound probe. D1: Complex between a RepA dimer and the operator sequence. D2: Complex including a second RepA dimer bound (13). W: RepA-DNA aggregates that stay in the well. ***B***, Titration of a radiolabelled fragment (0.10 nM) comprising the four origin iterons. F: Unbound DNA. M1-M4: Complexes including 1-4 RepA monomers bound to 1-4 iteron sequences (14). W: Larger RepA-DNA complexes in the well. Protein concentrations (nM) in both experiments: *Lane 1*, 7.5; *lane 2*, 18.8; *lane 3*, 47.2; *lane 4*, 117.3; *lane 5*, 293.1; *lane 6*, 732.9.

Fig. 4. **The molecular masses of the distinct RepA species determined by sedimentation equilibrium**. Symbols represent the experimental gradients (U.V. absorption of the sample *vs*. radial position in the centrifuge cell) at sedimentation equilibrium for 5 $\mu$M of: ***A***, RepA-WT;

***B***, His6-RepA-WT; and ***C***, His6-RepA-2L2A. Solid lines are the best fit gradients for single sedimenting species with molecular masses 53, 58 and 29 kDa, respectively. Dashed lines show the theoretical gradients of the monomer and dimer species of the three RepA proteins.

Fig. 5. **Steady state fluorescence spectroscopy highlights differences in the folds of His6 tagged RepA-WT and 2L2A mutant**. ***A***, Fluorescence emission spectra (λexcit= 295 nm) of Trp94 in RepA-WT and RepA-2L2A (both at 5 $\mu$M), whose association states and domain compactness are represented schematically. Dotted vertical lines indicate the emission maxima for the WT (327 nm) and mutant (348 nm) proteins. ***B***, Fluorescence emission spectra (λexcit= 395 nm) for the extrinsic fluorophore bis-ANS (10 $\mu$M) incubated with either RepA-WT or RepA-2L2A proteins at the same experimental conditions assayed in A. Dashed vertical line marks the emission maximum at 472 nm.

Fig. 6. **Iteron DNA as an allosteric effector on both RepA structure and association state**. ***A***, Near and far U.V. CD spectra of dsDNA oligonucleotides (5 $\mu$M, filled symbols) and their complexes with equimolar amounts of His6 tagged RepA-WT (empty symbols): inversely-repeated operator (1IR, in red), directly-repeated iteron (1DR, in blue) and unrelated yeast telomeric (TEL, in green) sequences. ***B***, Far U.V. CD spectra of His6-RepA-WT and 2L2A proteins at 5 $\mu$M (circles), plotted together with the result (diamonds) of subtracting the spectra of naked DNAs to the protein-DNA complexes. ***C***, HPLC gel filtration elution profiles of duplicates of the samples in A, maintaining the same colour and symbol codes. Drawings close to the peaks interpret the different DNA fragments and their complexes with His6-RepA-WT. *Inset* shows the sedimentation coefficient distributions calculated for both protein-DNA complexes, which were spun-down in an analytical ultracentrifuge just after peak elution.

Fig. 7. **Binding to operator or iteron DNAs increases the thermal stability of His6-RepA-WT**. Thermal denaturation profiles were acquired for duplicates of the samples in Fig. 6 (the same colours and symbols are adopted), measuring the evolution of molar ellipticity [θ] at 228 nm (protein secondary structure) with increasing temperature. *Inset table* contains thermodynamic parameters calculated from the curves. Tm: Temperature for half transition between folded (low θ values) and unfolded (θ getting close to 0) states. ΔTm: Variation of the melting temperature of His6-RepA-WT in the complexes with DNA, compared with that for the protein alone.

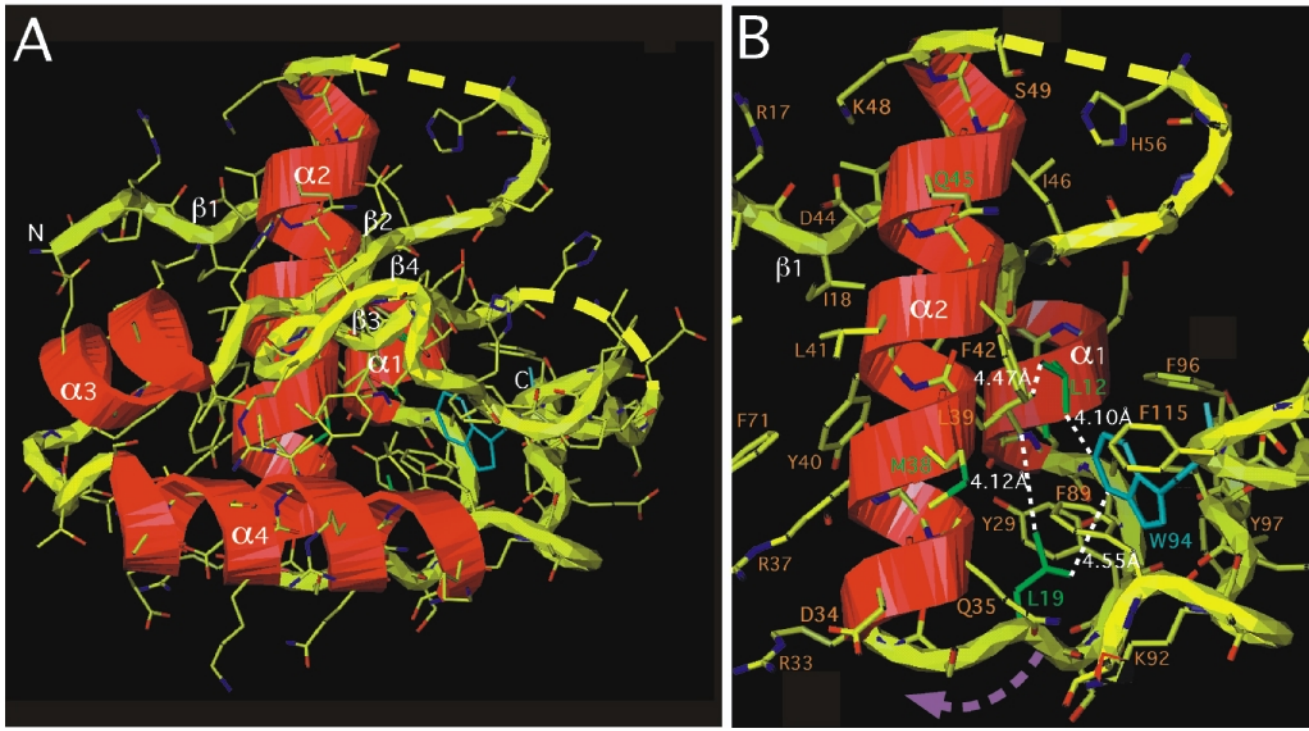
A
α2
β1
β2
β4
β3
α1
N
C
α3
α4
B
S49
R17
K48
H56
Q45
I46
D44
β1
I18
α2
L41
F42
α1
4.47Å
L12
F96
F71
L39
4.10Å
F115
Y40
M38
4.12Å
F89
Y29
W94
Y97
R37
4.55Å
D34
Q35
L19
R33
K92

Fig. 1

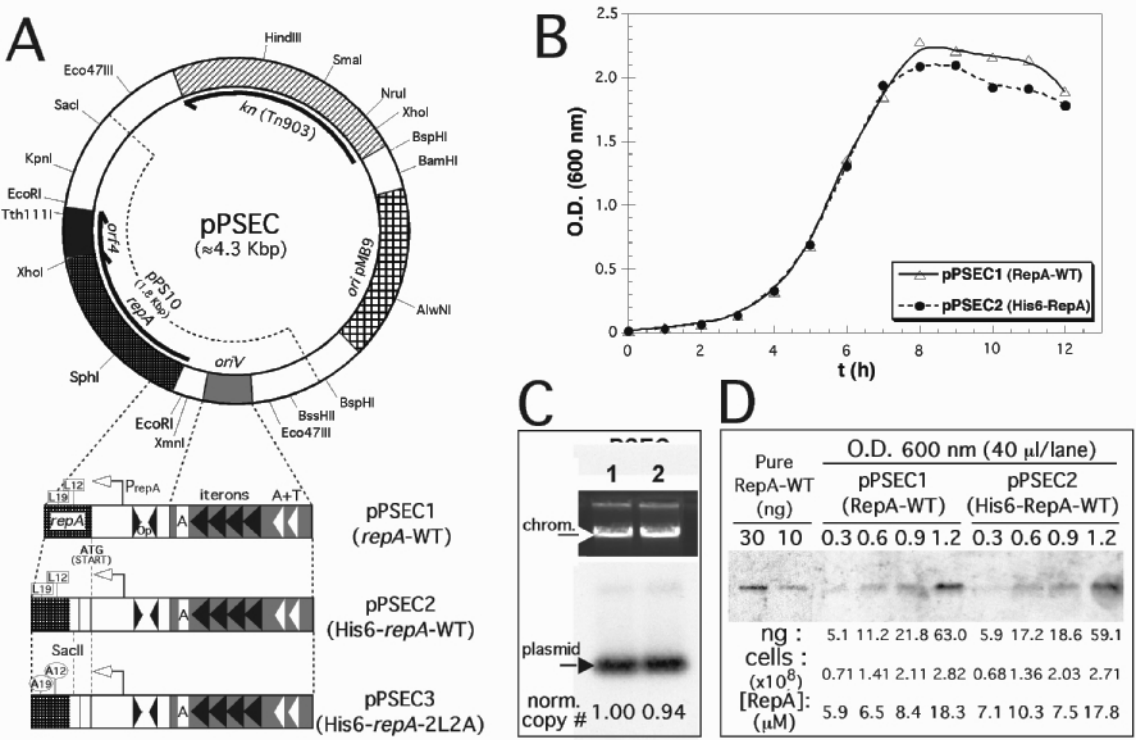
A
HindIII
SmaI
NruI
XhoI
BspHI
BamHI
AlwNI
BspHI
BssHII
Eco47III
EcoRI
XmnI
SphI
XhoI
KpnI
EcoRI
Tth111I
SacI
Eco47III
kn (Tn903)
pPSEC
(≈4.3 Kbp)
ori pM69
oriV
repA
pPS10
(1.8 Kbp)
ori γ
PrepA
L12
L19
repA
Op
A
iterons
A+T
pPSEC1
(repA-WT)
ATG
(START)
pPSEC2
(His6-repA-WT)
SacII
A12
A19
pPSEC3
(His6-repA-2L2A)
B
O.D. (600 nm)
t (h)
pPSEC1 (RepA-WT)
pPSEC2 (His6-RepA)
C
1
2
chrom.
plasmid
norm.
copy # 1.00 0.94
D
Pure
RepA-WT
(ng)
O.D. 600 nm (40 μl/lane)
pPSEC1
(RepA-WT)
pPSEC2
(His6-RepA-WT)
30 10 0.3 0.6 0.9 1.2 0.3 0.6 0.9 1.2
ng : 5.1 11.2 21.8 63.0 5.9 17.2 18.6 59.1
cells : (x10^8) 0.71 1.41 2.11 2.82 0.68 1.36 2.03 2.71
[RepA]: (μM) 5.9 6.5 8.4 18.3 7.1 10.3 7.5 17.8

Fig. 2

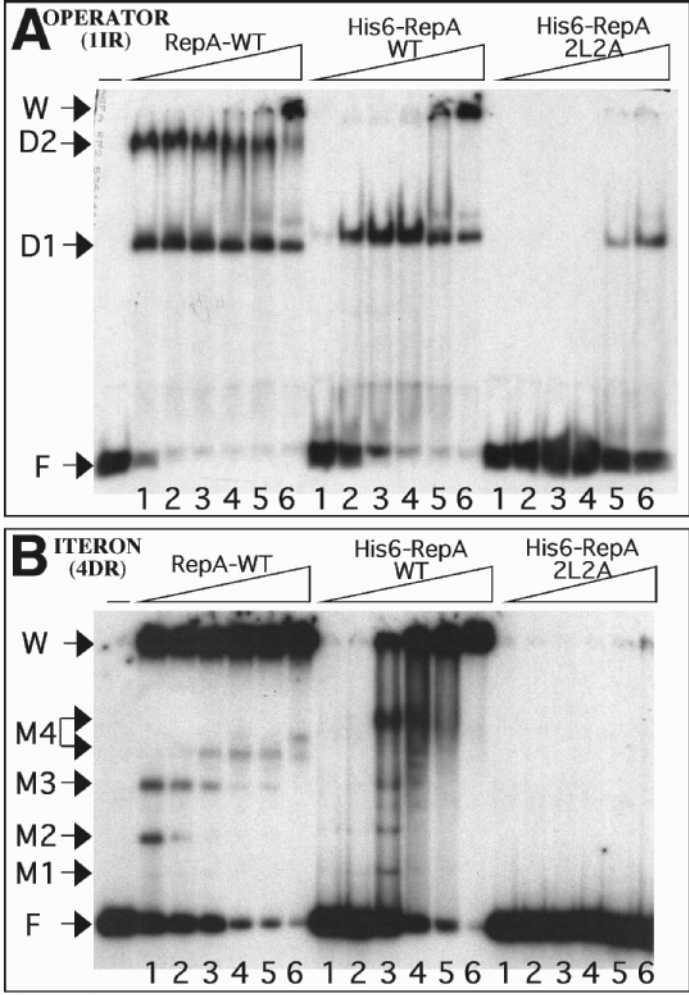
A
OPERATOR
(1IR)
RepA-WT
His6-RepA
WT
His6-RepA
2L2A
W
D2
D1
F
1 2 3 4 5 6 1 2 3 4 5 6 1 2 3 4 5 6
B
ITERON
(4DR)
RepA-WT
His6-RepA
WT
His6-RepA
2L2A
W
M4
M3
M2
M1
F
1 2 3 4 5 6 1 2 3 4 5 6 1 2 3 4 5 6

**Fig. 3**

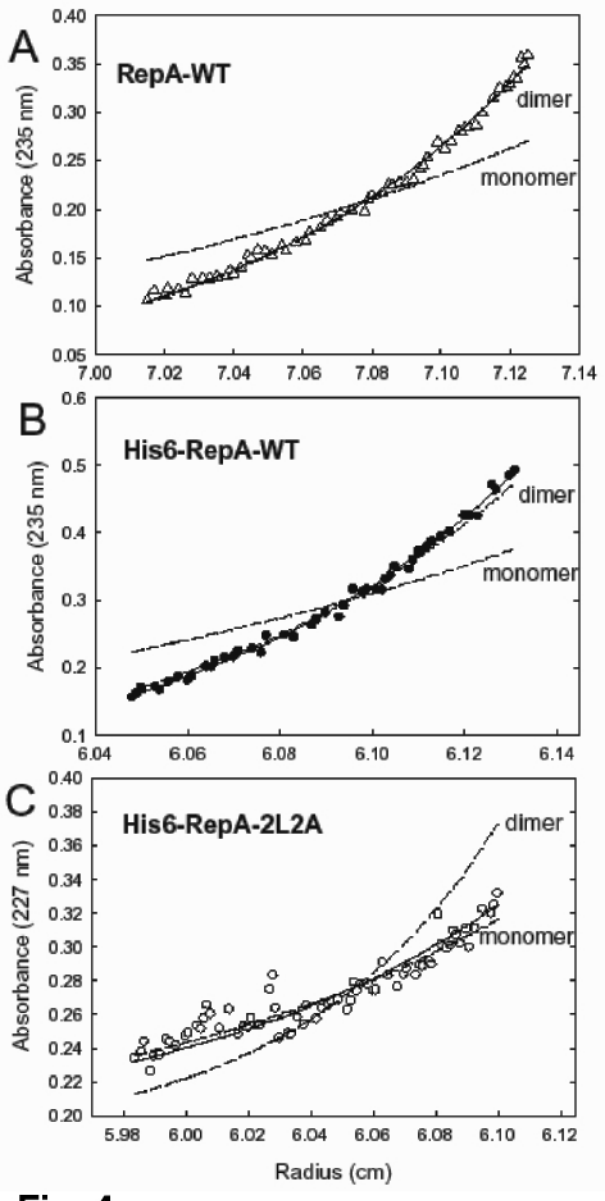
A
RepA-WT
dimer
monomer
Absorbance (235 nm)
0.40
0.35
0.30
0.25
0.20
0.15
0.10
0.05
7.00
7.02
7.04
7.06
7.08
7.10
7.12
7.14
B
His6-RepA-WT
dimer
monomer
Absorbance (235 nm)
0.6
0.5
0.4
0.3
0.2
0.1
6.04
6.06
6.08
6.10
6.12
6.14
C
His6-RepA-2L2A
dimer
monomer
Absorbance (227 nm)
0.40
0.38
0.36
0.34
0.32
0.30
0.28
0.26
0.24
0.22
0.20
5.98
6.00
6.02
6.04
6.06
6.08
6.10
6.12
Radius (cm)

**Fig. 4**

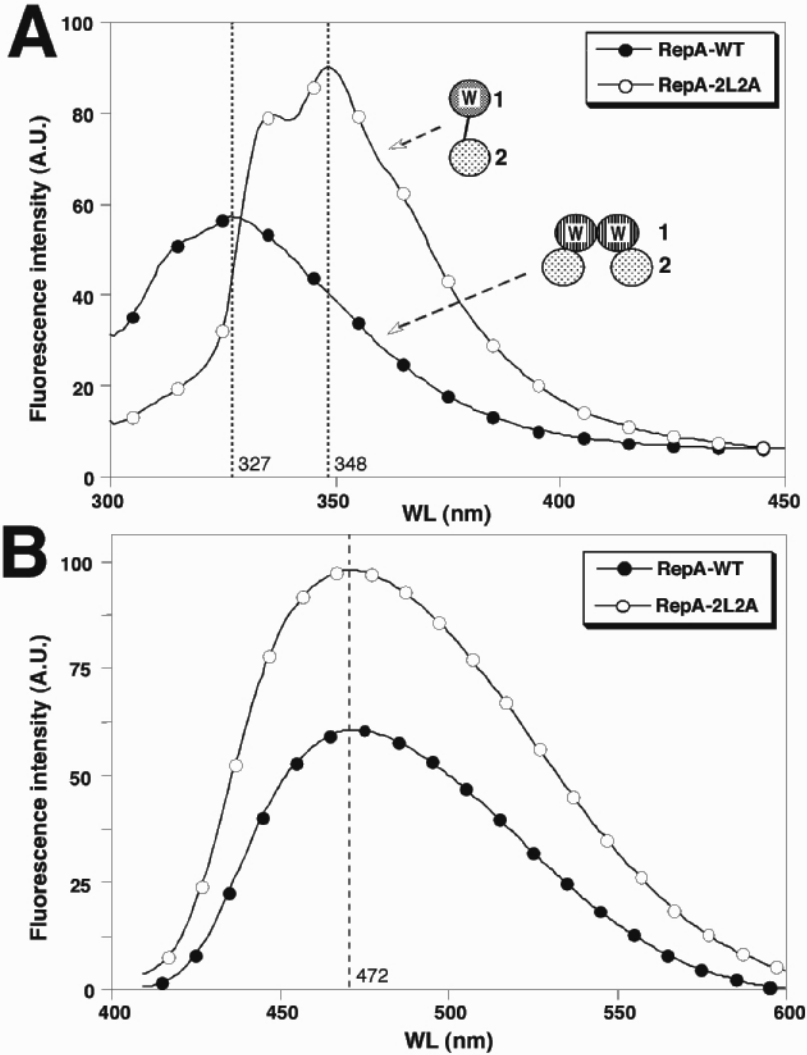
A
RepA-WT
RepA-2L2A
Fluorescence intensity (A.U.)
WL (nm)
327
348
W
1
2
B
RepA-WT
RepA-2L2A
Fluorescence intensity (A.U.)
WL (nm)
472

Fig. 5

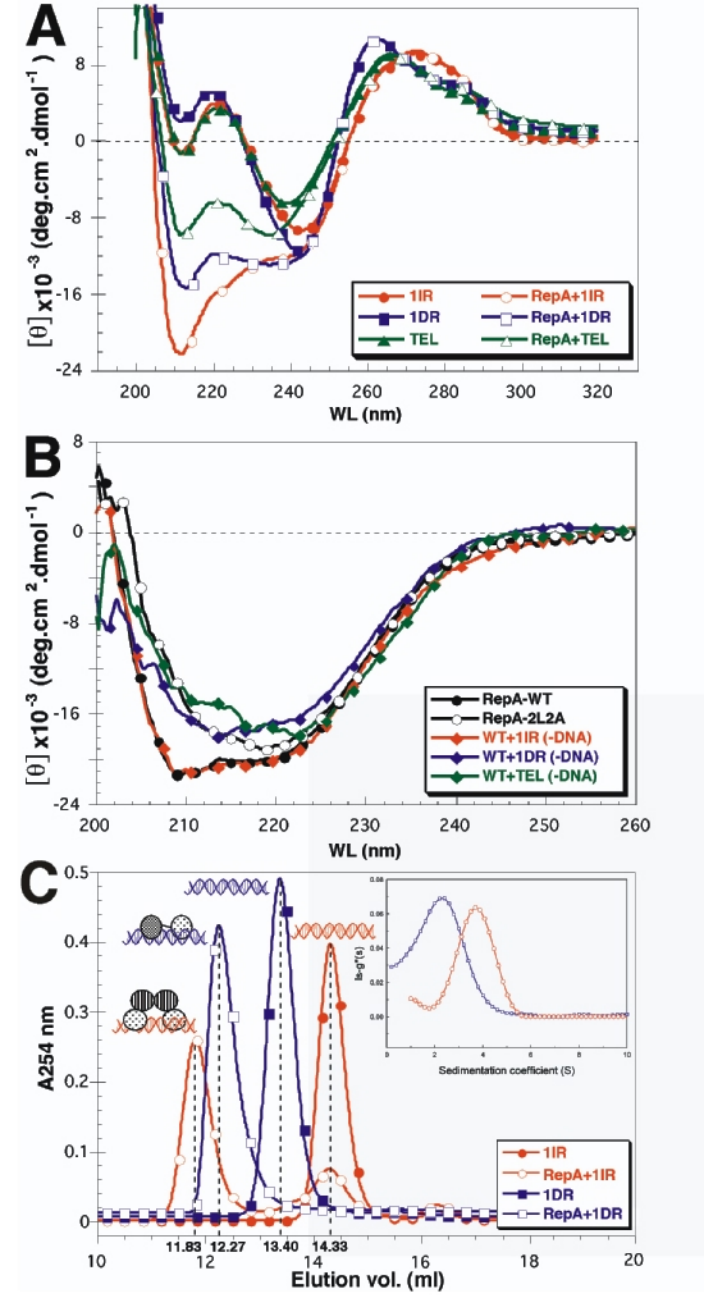
A
[θ] x10 -3 (deg.cm 2 .dmol -1 )
8
0
-8
-16
-24
200
220
240
260
280
300
320
WL (nm)
1IR
1DR
TEL
RepA+1IR
RepA+1DR
RepA+TEL
B
[θ] x10 -3 (deg.cm 2 .dmol -1 )
8
0
-8
-16
-24
200
210
220
230
240
250
260
WL (nm)
RepA-WT
RepA-2L2A
WT+1IR (-DNA)
WT+1DR (-DNA)
WT+TEL (-DNA)
C
A254 nm
0.5
0.4
0.3
0.2
0.1
0
10
12
14
16
18
20
Elution vol. (ml)
11.83
12.27
13.40
14.33
ls-g*(s)
Sedimentation coefficient (S)
1IR
RepA+1IR
1DR
RepA+1DR

Fig. 6

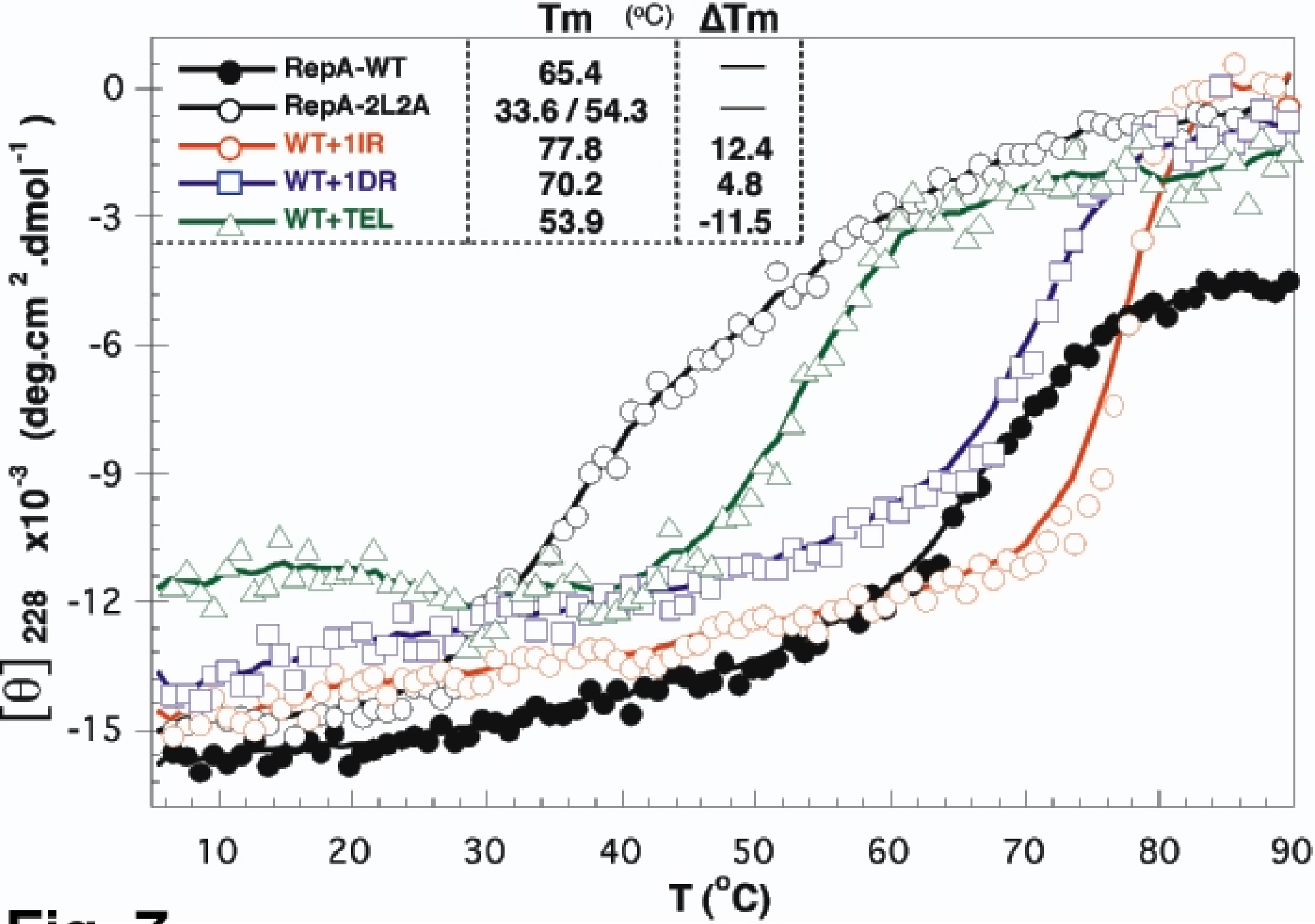
Tm (°C)
ΔTm
RepA-WT
RepA-2L2A
WT+1IR
WT+1DR
WT+TEL
65.4
33.6 / 54.3
77.8
70.2
53.9
—
—
12.4
4.8
-11.5
0
-3
-6
-9
-12
-15
[θ]228 x10-3 (deg.cm2.dmol-1)
10
20
30
40
50
60
70
80
90
T (°C)

Fig. 7